Shear strengthening effect by bonded GFRP strips and transverse steel on RC T-beams

K.C. Panda[*1], S.K. Bhattacharyya[2a] and S.V. Barai[3b]

[1]*Department of Civil Engineering, ITER, SOA University, Bhubaneswar, 751030, Odisha, India*
[2]*CSIR-Central Building Research Institute, Roorkee, 247667, Uttarakhand, India*
[3]*Department of Civil Engineering, IIT Kharagpur, 721302, West Bengal, India*

Abstract.   This study focuses on shear strengthening performance of simply supported reinforced concrete (RC) T-beams bonded by glass fibre reinforced polymer (GFRP) strips in different configuration, orientations and transverse steel reinforcement in different spacing. Eighteen RC T-beams of 2.5 m span are tested. Nine beams are used as control beam. The stirrups are provided in three different spacing such as without stirrups and with stirrups at a spacing of 200 mm and 300 mm. Another nine beams are used as strengthened beams. GFRP strips are bonded in shear zone in U-shape and side shape with two types of orientation of the strip at 45° and 90° to the longitudinal axis of the beam for each type of stirrup spacing. The experimental result indicates that the beam strengthened with GFRP strips at 45° orientation to the longitudinal axis of the beam are much more effective than 90° orientation. Also as transverse steel increases, the effectiveness of the GFRP strips decreases.

Keywords: glass fibre reinforced polymer (GFRP); reinforced concrete (RC); strengthening; shear strength; T-beams

1. Introduction

Several studies demonstrated that strengthening of reinforced concrete structures using externally bonded fibre reinforced plastic sheets and strips is an effective method to enhance the structural performance. The high strength and stiffness-to-weight ratio of fibre reinforced polymer (FRP) composites allow the use of these materials in construction for repairing and retrofitting of damaged structures, or strengthening of undamaged structures to enhance the load carrying capacities. Generally beams are strengthened for both flexural and shears strength. Common methods of strengthening of RC beams include side bonding, U-jacketing and full wrapping. Research studies on shear strengthening with FRP are sparse and are mostly limited to relatively small beams and it is still under investigation. The research in this area exists since 1992 (Berset 1992).

The analytical studies on shear strength models of RC beams with externally bonded FRP is

---

∗Corresponding author, Associate Professor, E-mail: kishoriit@gmail.com
[a]Director, E-mail: sriman_bhattacharyya@yahoo.com
[b]Professor, E-mail: skbarai@civil.iitkgp.ernet.in

discussed by various authors (e.g., Chaallal *et al*. 1998, Triantafillou 1998, Triantafillou and Antonopoulos 2000, Khalifa *et al*. 1998, Chen and Teng 2003a, b). These models basically provided design, detailing, and installation guidelines for FRP strengthening. Chen *et al*. (2010b) has recently demonstrated that adverse interaction between external FRP shear reinforcement and internal steel shear reinforcement may significantly affect the effectiveness of FRP shear strengthening for the debonding failure mode, especially when side strips are used. However, the effect of such shear interaction is not appropriately reflected in existing shear strength models for RC beams strengthened for shear with FRP (Chen 2010). The development of shear contribution of steel stirrups with the crack width has been numerically investigated by Chen *et al*. (2010b). Chen *et al*. (2012) presented an analytical study on the progressive debonding of FRP strips in such strengthened beams. The complete debonding process was modeled and the contribution of the FRP strips to the shear capacity of the beam was quantified. The experimental studies on RC rectangular beams, strengthened with FRP in shear have been carried out by several researchers (Al-Sulaimani *et al*. 1994, Noris *et al*. 1997, Li *et al*. 2001, Khalifa and Nanni 2002, Pellegrino and Modena 2002, Taljsten 2003, Zhang and Hsu 2005, Adhikary *et al*. 2004, Cao *et al*. 2005, Mosallam and Banerjee 2007, Leung *et al*. 2007, Maaddawy and Sherif 2009, Sundarraja and Rajamohan 2009, EI-Ghandour 2011). Similarly, the experimental studies on RC T-beams, strengthened with FRP in shear have been contributed by (Chajes *et al*. 1995, Khalifa and Nanni 2000, Deniaud and Cheng 2001, 2003, Hag-Elsafi *et al*. 2001, Chaallal *et al*. 2002, Micelli *et al*. 2002, Bousselham and Chaallal 2006, 2008, Monti and Liotta 2007, Kim *et al*. 2008, Le and Al-Mahaidi 2008, Belarbi *et al*. 2012, Lee *et al*. 2011). The researchers have shown that the shear strength of RC beams may be substantially increased by bonding fibre reinforced polymer (FRP) strips or sheets as external shear reinforcement. Most of the experimental works have been conducted using CFRP as external shear reinforcement both for rectangular and T-beams, as compared with GFRP as external shear reinforcement. The works using GFRP as strengthening material are very limited both for rectangular (Al-Sulaimani *et al*. 1994, Cao *et al*. 2005) and T-beams (Chajes *et al*. 1995, Deniaud and Cheng 2001, 2003, Panda *et al*. 2010, 2011, 2012, 2013). This paper presents an experimental study on the effectiveness, modes of failure and strain analysis of RC T-beams strengthened in shear using epoxy bonded GFRP strips in different configurations and orientations.

2. Theoretical study

Shear strengthening of RC beams are influenced by many factors such as size and geometry of the beam, the strength of concrete, internal shear and flexural reinforcements, loading conditions, the method of strengthening, and the properties of the bonded FRP. All the existing models used the same expression as given in Eq. (1), to calculate the shear strength of a strengthened RC beam.

$$V_n = V_c + V_s + V_f \tag{1}$$

Where V_c is the shear capacity of the concrete which consists of shear contributions of concrete in compression, aggregate interlock and dowel action of steel flexural reinforcement, V_s is the contribution of the steel stirrups and bent up bars and V_f is the contribution of the FRP, V_c and V_s may be calculated according to provisions in existing design codes, so the main difference between available models lie in the evaluation of the FRP contribution V_f.

Khalifa *et al*. (1998) used a slight modification of Chaallal *et al*. (1998) model by calibrating more test results to describe shear failure combined simultaneously with FRP rupture and bond model of Maeda *et al*. (1997) to describe shear failure combined with FRP debonding. These two models were presented in ACI shear design format.

2.1 Design approach based on effective FRP stress

The equation presented by Triantafillou (1998), in the Euro code format as in Eq. (2).

$$V_f = \frac{0.9}{\gamma_f} \rho_f E_f \varepsilon_{fe} b_w d \left(1 + \cot \beta\right) \sin \beta \qquad (2)$$

Eq. (2) was slightly modified by Khalifa *et al*. (1998) in ACI 440.2R-02 guidelines as in Eq. (3) and also used in the present study to get the shear contribution of GFRP strips in strengthened T-beams.

$$V_f = \frac{A_f f_{fe} \left(\sin \beta + \cos \beta\right) d_f}{s_f} \qquad (3)$$

Where f_{fe} is the effective GFRP stress, d_f is the effective depth of the GFRP shear reinforcement, and s_f is the spacing of GFRP strips. For continuous vertical shear reinforcement, the spacing of the strip, s_f, and the width of the strip, w_f, are equal. The dimensions used to define the area of GFRP are as shown in Figs. 1 and 2. GFRP shear reinforcement ratio for strips and continuous sheet is given in Eqs. (4) and (5).

$$\rho_f = \text{GFRP shear reinforcement ratio} = \left(\frac{2t_f}{b_w}\right)\left(\frac{w_f}{s_f}\right) \text{ (for strips)} \qquad (4)$$
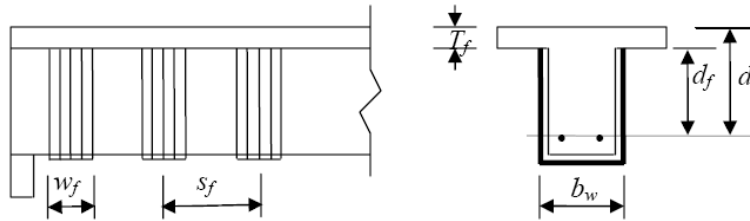

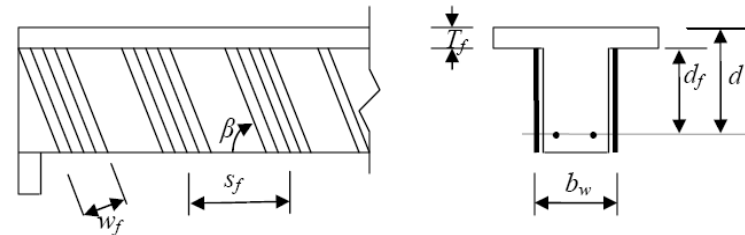Fig. 1 Dimensions used to define the area of GFRP for vertically oriented strips

Fig. 2 Dimensions used to define the area of GFRP for inclined oriented strips

$$\rho_f = \text{GFRP shear reinforcement ratio} = \left(\frac{2t_f}{b_w}\right) \text{ (for continuous sheets)} \qquad (5)$$

2.2 Modification to effective strain model

Khalifa *et al*. (1998) modified the effective strain model by including additional experimental data to the model presented by Triantafillou (1998). The modified new model based on the observation that $\rho_f E_f$ does not exceed 1.1 GPa.

To eliminate the effects of various types of FRP sheet, the ratio of effective strain to ultimate strain, $R = \dfrac{\varepsilon_{fe}}{\varepsilon_{fu}}$, was plotted versus axial rigidity. Regression of experimental data led to the following expression i.e., the polynomial was used as a best fit to the data in the case of $\rho_f E_f < 1.1$ GPa. This polynomial is given in Eq. (6).

$$R = 0.5622\left(\rho_f E_f\right)^2 - 1.2188\left(\rho_f E_f\right) + 0.778 \leq 0.50 \qquad (6)$$

The upper limit of *R* was 0.5; this limit was suggested to maintain the shear integrity of concrete. The ratio of effective strain to ultimate strain, *R*, may be used as a reduction factor on the ultimate strain. The proposed equation is not considered the strength of the concrete and bonded surface configuration. The Eq. (6) is calibrated from the test results of both CFRP rupture and delamination. Khalifa *et al*. (1998) claimed it should only be used to calculate the reduction factor for FRP sheet rupture not by FRP sheet delamination.

2.3 Reduction coefficient based on debonding failure mode

The reduction coefficient based on debonding failure mode, is given in ACI 440.2R-02 design approach, is slightly modified from Khalifa's approach. k_v is used as bond reduction coefficient. The analytical result of present study is based on ACI design approach.

The bond-reduction coefficient is a function of the concrete strength, the type of wrapping scheme used and the stiffness of the laminate. The bond reduction coefficient may be computed using Eqs. (7) through (10).

$$k_v = \frac{k_1 k_2 L_e}{11{,}900\varepsilon_{fu}} \leq 0.75 \qquad (7)$$

The active bond length L_e is the length over which the majority of the bond stress is maintained. This length is given by Eq. (8).

$$L_e = \frac{416}{\left(nt_f E_f\right)^{0.58}} \qquad (8)$$

The bond-reduction coefficient also relies on two modification factors, k_1 and k_2, that account for the concrete strength and the type of wrapping scheme used, respectively. Expressions for these modification factors are given in Eqs. (9)-(10).

$$k_1 = \left(\frac{f_c'}{27}\right)^{2/3} \tag{9}$$

$$k_2 = \frac{d_f - L_e}{d_f} \text{ for U-wraps and } k_2 = \frac{d_f - 2L_e}{d_f} \text{ for two sides bonded} \tag{10}$$

Where, f_c' and E_f are in MPa.

2.4 Reinforcement limits

The total shear reinforcement should be taken as sum of the contribution of the GFRP shear reinforcement and the steel shear reinforcement. The total shear reinforcement should be limited based on the criteria given for steel alone in ACI 318-99 section as stated in Eq. (11).

$$V_s + V_f \le 0.66\sqrt{f_c'}\, b_w d \tag{11}$$

3. Experimental investigation

The parameters selected for the experimental investigation are the followings:
(a) Three T-beam specimens without transverse steel (stirrups) but with GFRP strips having U-shape, and side bonded with orientation at 45° and 90° with respect to the longitudinal axis of the beam.
(b) Three T-beam specimens with transverse steel (stirrups) spaced at 300 mm c/c and with GFRP strips having U-shape, and side bonded with orientation at 45° and 90° with respect to the longitudinal axis of the beam.
(c) Three T-beam specimens with transverse steel (stirrups) spaced at 200 mm c/c and with GFRP strips having U-shape, and side bonded with orientation at 45° and 90° with respect to the longitudinal axis of the beam.

3.1 Details of test specimens

The experimental program consists of eighteen (18) simply supported RC T-beams. Nine (9) beams are tested as control beam and the rest nine beams are tested as strengthened beam. All the T-beams are 2.5 m long having 250 mm flange width and 60 mm thickness, 100 mm wide web and 200 mm deep and designed to fail in shear as per IS 456: 2000. Based on the design, two Nos. 20 mm diameter Tor steel bars are used as flexural reinforcement (area 628.31 mm^2) at the bottom, and four Nos. 8 mm diameter Tor steel bars are used in one layer at the top. The internal steel stirrups are 6 mm diameter. Nine control beams are tested in three different series. The first series, without stirrups, only the stirrups are provided at the support and the loading points to avoid the local shear failure. The second series of control specimen, the spacing of the stirrups are 300 mm c/c, whereas in third series, the spacing of the stirrups is 200 mm c/c. The other nine beams are strengthened in shear with GFRP strips in shear span in two different configurations such as side bonded and U-shape. Whereas in side bonded configuration the orientation of the GFRP strip is provided at 45° and 90° to the longitudinal axis of the beam for each type of stirrups spacing. The

Table 1 Detail of test specimens of control and strengthened RC T-Beams

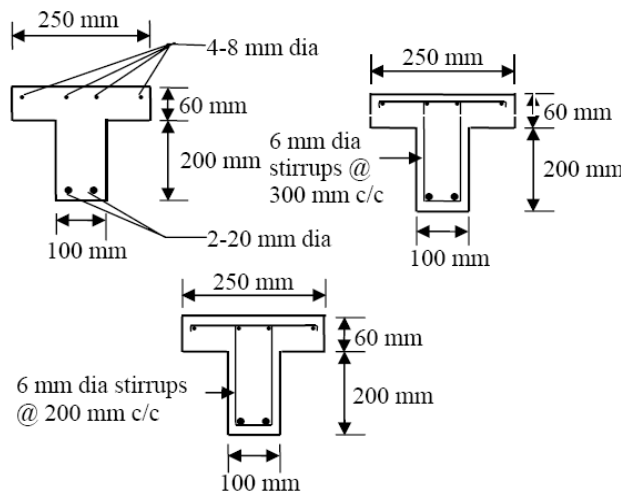| Specimen Designation	Strengthening schemes
S0-0L	Control beam without transverse steel (Stirrups)
S300-0L	Control beam with transverse steel (Stirrups at a spacing of 300 mm c/c)
S200-0L	Control beam with transverse steel (Stirrups at a spacing of 200 mm c/c)
S0-1L-ST-U-90	Without stirrups + one layer of GFRP strips in the form of U-shape + 90° orientation to the longitudinal axis of the beam
S0-1L-ST-S-90	Without stirrups + one layer of GFRP strips in the form of side bonded + 90° orientation to the longitudinal axis of the beam
S0-1L-ST-S-45	Without stirrups + one layer of GFRP strips in the form of side bonded + 45° orientation to the longitudinal axis of the beam
S300-1L-ST-U-90	With stirrups @ 300 mm c/c + one layer of GFRP strips in the form of U-shape + 90° orientation to the longitudinal axis of the beam
S300-1L-ST-S-90	With stirrups @ 300 mm c/c + one layer of GFRP strips in the form of side bonded + 90° orientation to the longitudinal axis of the beam
S300-1L-ST-S-45	With stirrups @ 300 mm c/c + one layer of GFRP strips in the form of side bonded + 45° orientation to the longitudinal axis of the beam
S200-1L-ST-U-90	With stirrups @ 200 mm c/c + one layer of GFRP strips in the form of U-shape + 90° orientation to the longitudinal axis of the beam
S200-1L-ST-S-90	With stirrups @ 200 mm c/c + one layer of GFRP strips in the form of side bonded + 90° orientation to the longitudinal axis of the beam
S200-1L-ST-S-45	With stirrups @ 200 mm c/c + one layer of GFRP strips in the form of side bonded + 45° orientation to the longitudinal axis of the beam

Fig. 3 Details of control specimen

strengthened specimen designated as S0-1L-ST-S-45 indicates without steel stirrup (S0), strengthened with one layer of GFRP (1L) strip (ST), bonded on the sides of the web of T-beams (S), and orientation of the fibre angle is at 45º to the longitudinal axis of the beam. The details of the specimens are listed in Table 1. The control specimen details and dimensions are as shown in Fig. 3.

Table 2 Test results of cubes and cylinders after 28 days

Specimen Designation	No. of Beams	Mean cube compressive strength (MPa)	Mean cylinder compressive strength (MPa)	Split tensile strength of cylinder (MPa)	Modulus of elasticity as per test results (MPa)
S0-0L	3	49.61	42.16	NA	3.465×10^4
S200-0L	3	59.78	42.67	NA	NA
S300-0L	3	57.62	39.53	2.70	3.624×10^4
S0-1L-ST-S-90	1				
S0-1L-ST-S-45	1	52.18	40.03	2.68	4.264×10^4
S0-1L-ST-U-90	1				
S200-1L-ST-S-90	1				
S200-1L-ST -S-45	1	53.62	37.83	2.55	3.915×10^4
S200-1L-ST -U-90	1				
S300-1L-ST -S-90	1				
S300-1L-ST -S-45	1	51.03	38.28	2.63	3.215×10^4
S300-1L-ST -U-90	1				

Table 3 Mechanical properties of steel reinforcement

Material	Diameter (mm)	Yield stress (MPa)	Ultimate stress (MPa)	Modulus of elasticity (GPa)	Yield strain (μ strains)
Tor steel	20	500	590	200	2500
Tor steel	8	503	646	180	2794
Mild steel	6	252	461	200	-

Table 4 Mechanical properties GFRP

Characteristics of coupon test	Value obtained experimentally for single sample
Width, mm	19.4
Thickness, mm	1.0
Area, mm^2	19.4
Modulus, MPa	13300
Ultimate, kN	3.14
Ultimate, MPa	161.85
TE, %	1.220
Break, %	1.220
Yield, %	1.100
Ultimate, %	1.217

3.2 Materials used

Ordinary Portland Cement (OPC-43 grade) and 12.5 mm downgraded coarse aggregates are used for the preparation of concrete. The Mix design is carried out for M30 grade of concrete. The design proportions of the ingredients namely cement, fine aggregate, and coarse aggregate are (1:0.946:2.03). The water cement ratio by weight is 0.375. The slump tests are conducted for each batch of mixing, the slump values are varying between 30-50 mm. Compression tests on cubes and cylinders are performed at 7 days and 28 days. The modulus of elasticity and split tensile strength
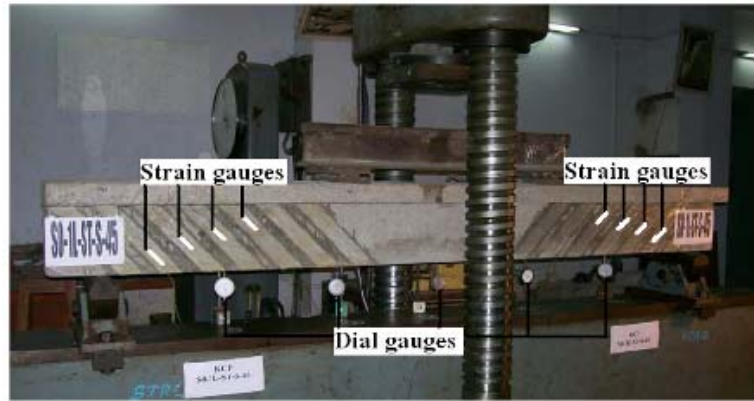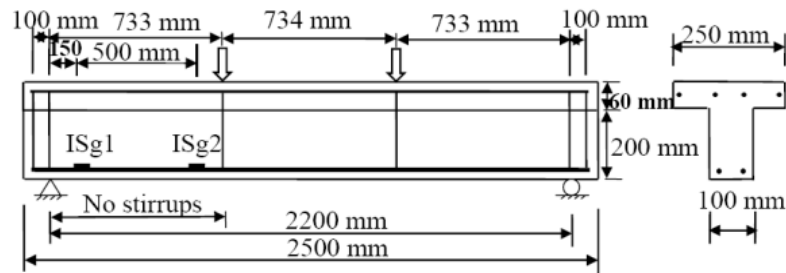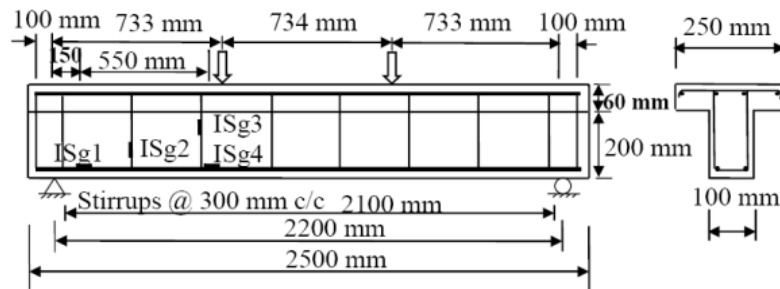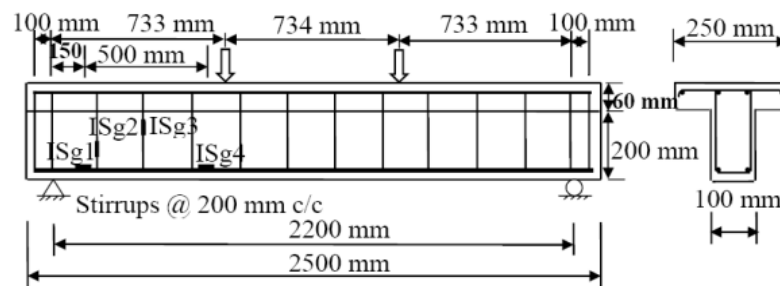
Fig. 4 Details of the test setup

(a) Internal strain gauge locations in S0-Series

(b) Internal strain gauge locations in S300-Series

(c) Internal strain gauge locations in S200-Series

Fig. 5 Location of internal strain gauges in longitudinal and transverse steel

is also determined. The test results of cubes and cylinders are presented in Table 2.

The steel reinforcements used are also tested in the laboratory according to the Indian Standards. Steels of grade Fe 415 for longitudinal reinforcement and Fe 250 for transverse reinforcement are used in the experiment. The summary of test results is presented in Table 3.

GFRP strips of thickness 0.36 mm and width 50 mm is used for strengthening of the beams. The resin used is a 9:1 mixture of Araldite CY-230 and hardener HY-951. The ultimate tensile strength of the GFRP strip is measured 160 MPa and the elastic modulus is 13.18 GPa. The properties of coupon test results are presented in Table 4.

3.3 Instrumentation and test procedure

All the beams are tested using two points loading with shear span (a) to effective depth (d) ratio equal to 3.26. The tests are carried out at the structural laboratory of Civil Engineering Department, IIT Kharagpur using 300 T Universal Testing Machine (UTM). Fig. 4 shows the details of the test setup.

Five dial gauges are used to monitor vertical displacements. One dial gauge is placed at the midspan of the beam. Two dial gauges are placed below the loading points and another two are located at the center of the shear zone on either side as shown in Fig. 4.

Two types of electrical strain gauges are used in the present study. BKNIC-10 strain gauge (Gauge length 10 mm, Gauge factor 2.00 ± 2 %, Resistance 355.0 ± 0.5 Ω) is placed on the surface of the longitudinal and transverse steel reinforcement. BKCT-30 strain gauge (Gauge length 30 mm, Gauge factor 2.00 ± 2 %, Resistance 350.5 ± 0.5 Ω) is placed on the concrete surface. BKNIC-10 is attached on the longitudinal steel and transverse steel to measure strain during the different stages of loading. Fig. 5 shows the details of the internal strain gauge locations in longitudinal and transverse steel.

BKCT-30 gauges are attached on the side of the beam web and to the GFRP strips on the side of the strengthened T-beams and oriented in the fibre direction. Eight strain gauges are attached on the GFRP strips at the locations on the expected plane of the shear cracks on both sides of the strengthened T-beams. Four strain gauges are attached on each side crack on the assumed path of the control beam. The coordinates of strain gauge locations from the left support considering bottom corner as (0, 0) in strengthened beam for Sg1, Sg2, Sg3, and Sg4 are (150, 50), (250, 100), (350, 100), and (450, 150) respectively. Similarly, the coordinates for Sg5, Sg6, Sg7, and Sg8 are used from right support. The details of surface strain gauge positions are shown in Fig. 6.

4. Analysis of results and discussions

Table 5 shows the experimental data on shear strengthening using GFRP strips. Also the GFRP shear reinforcement ratio (ρ_f), transverse steel reinforcement ratio (ρ_s), longitudinal steel reinforcement ratio (ρ_w) and effective GFRP strain (ε_{fe}) of all the specimens are presented in Table 5. The modes of failure as observed in the experimental study are also indicated. The experimental shear strength results are presented in Table 6. The different nomenclatures used in the Table 6 are explained herein for clarity. $V_{n,test}$ = Total nominal shear strength by test, $V_{c,test}$ = nominal shear strength provided by concrete obtained from test, $V_{s,test}$ = nominal shear strength provided by steel shear reinforcement obtained from test, $V_{f,test}$ = nominal shear strength provided by GFRP obtained from test, whereas $V_{n,theor}$ = nominal shear strength calculated theoretically using ACI guidelines,
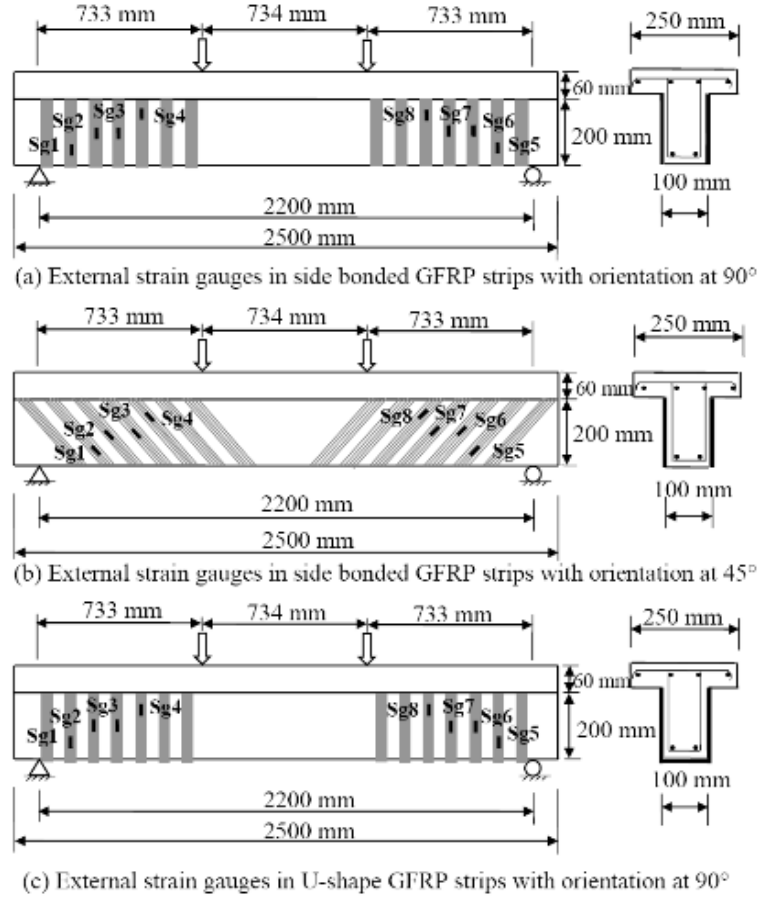
Fig. 6 Location of surface strain gauges on strengthened T-beams

$V_{c,theor}$ = nominal shear strength provided by concrete theoretically, $V_{s,theor}$ = nominal shear strength provided by steel shear reinforcement theoretically, $V_{f,theor}$ = nominal shear strength provided by GFRP theoretically. In S0-0L specimen, there is no stirrups are present in the shear zone, $V_{n,test}$ and $V_{c,test}$ both are equal and the value is 50 kN. In S300-0L and S200-0L specimens the $V_{n,test}$ values are 70.5 kN and 80 kN respectively. As stirrups are present, the contribution of stirrups from the respective specimens obtained by the difference between the $V_{n,test}$ of S300-0L and S200-0L specimen and $V_{c,test}$ of S0-0L specimen. $V_{s,test}$ value for S300-0L and S200-0L specimens are 20.5 kN and 30 kN respectively. As strengthened beam is concerned, $V_{n,test}$ value of S0-1L-ST-S-90 is 58 kN. The shear strength contribution of GFRP strip of specimen S0-1L-ST-S-90 i.e. $V_{f,test}$ value is obtained by deducting $V_{n,test}$ value of S0-0L specimen from the $V_{n,test}$ value S0-1L-ST-S-90 specimen, the value is 8 kN. Similarly, $V_{f,test}$ value obtained for S0-1L-ST-S-45 and S0-1L-ST-U-90 specimens is 23 kN and 12 kN respectively. As GFRP strips and transverse steel reinforcement both are concerned i.e for S300 and S200 series, $V_{f,test}$ value is obtained by deducting $V_{n,test}$ of control specimen from $V_{n,test}$ of strengthened specimen of the same series. Let's take S300-1L-ST-S-90 specimen. $V_{n,test}$ value is 77 kN, $V_{n,test}$ value of control specimen S300-0L is 70.5. $V_{f,test}$ value is

Table 5 Experimental data on shear strengthening using GFRP strip

Specimen	Config.	b_w	d	a/d	t_f	ρ_f	ρ_s	ρ_w	ε_{fu}	ε_{fe}	E_f	Modes of failure
		mm	mm		mm	%	%	%	10^{-3}	10^{-3}	GPa	
S0-0L	0	100	225	3.26	-	-	-	2.79	-	-	-	Shear failure
S300-0L	0	100	225	3.26	-	-	0.19	2.79	-	-	-	Shear failure
S200-0L	0	100	225	3.26	-	-	0.28	2.79	-	-	-	Shear failure
S0-1L-ST-S-90	S-90	100	225	3.26	0.36	0.36	-	2.79	12.14	8.884	13.18	GFRP debonding
S0-1L-ST-S-45	S-45	100	225	3.26	0.36	0.42	-	2.79	12.14	9.932	13.18	GFRP debonding and rupture
S0-1L-ST-U-90	U-90	100	225	3.26	0.36	0.36	-	2.79	12.14	9.076	13.18	GFRP debonding and rupture
S300-1L-ST-S-90	S-90	100	225	3.26	0.36	0.36	0.19	2.79	12.14	7.497	13.18	GFRP debonding
S300-1L-ST-S-45	S-45	100	225	3.26	0.36	0.42	0.19	2.79	12.14	7.917	13.18	GFRP debonding and rupture
S300-1L-ST-U-90	U-90	100	225	3.26	0.36	0.36	0.19	2.79	12.14	9.450	13.18	GFRP debonding and rupture
S200-1L-ST-S-90	S-90	100	225	3.26	0.36	0.36	0.28	2.79	12.14	7.548	13.18	GFRP debonding
S200-1L-ST-S-45	S-45	100	225	3.26	0.36	0.42	0.28	2.79	12.14	7.716	13.18	GFRP debonding and rupture
S200-1L-ST-U-90	U-90	100	225	3.26	0.36	0.36	0.28	2.79	12.14	8.978	13.18	GFRP debonding

obtained by deducting $V_{n,test}$ value of control specimen from $V_{n,test}$ value of strengthened specimen, the value is 6.5 kN. Similarly, the $V_{f,test}$ value can be obtained for other strengthened specimens.

4.1 Strength

It is observed from Table 6, in S0 series, for specimen S0-1L-ST-S-90, the load at ultimate failure is 116 kN, compared to 100 kN for S0-0L specimen. This indicates that there is a gain of 16%. As for the influence of the GFRP configuration and orientation on the gain in strength, that is for S0-1L-ST-U-90 and S0-1L-ST-S-45 the loads at ultimate failure are 124 kN and 146 kN respectively. The percentage gain is 24% and 46% respectively on loads over control specimen S0-0L. As expected without transverse steel reinforcement, the beams strengthened with GFRP side strips perpendicular to the diagonal shear cracks outperformed those strengthened with vertical GFRP strips 90° to the longitudinal axis of the beam. In S300 series, it is observed that for specimen S300-1L-ST-S-90, the load at ultimate failure is 154 kN, compared to 141 kN for control specimen S300-0L. A percentage gain in strength of 9.22% is observed. As for the influence of the GFRP configuration and orientation on the gain in strength, that is for S300-1L-ST-U-90 and S300-1L-ST-S-45 the loads at ultimate failure are 164 kN and 166 kN respectively. The percentage gain in strength for these two specimens are 16.31% and 17.73% respectively compared to the control specimen S300-0L. Whereas in S200 series, the loads at ultimate failure of S200-1L-ST-S-90, S200-1L-ST-U-90, and S200-1L-ST-S-45 specimens are 172 kN, 186 kN, and 182 kN respectively compared to 160 kN for control specimen S200-0L. This shows a gain of

7.5%, 16.25%, and 13.75% respectively on loads over control specimen. As expected with transverse steel reinforcement at 300 mm and 200 mm stirrup spacing, the beams strengthened with GFRP strips on side of the web of the T-beams at 45˚ orientation to the longitudinal axis of the beam and the beams strengthened with U configuration carry more loads than the other.

It is concluded from the three series that, the shear strength contribution of GFRP strips for different configurations and orientations, and without transverse steel reinforcements is relatively more effective than with strengthened RC T-beam with transverse steel reinforcements. The addition of internal transverse steel resulted in a significant decrease in shear capacity of the GFRP strips oriented in 45° direction as compared with no transverse steel reinforcements. Whereas in U-shape and side shape with orientation of the GFRP strip at 90°, the decrease in shear contribution of GFRP strip is less as compared with no transverse steel reinforcement.

4.2 Deflection

The variation of midspan deflection with load for the beams of series S0, S300, and S200 is shown in Fig. 7. It is observed from Fig. 7, the maximum deflection of S0-1L-ST-S-90, S0-1L-ST-S-45, and S0-1L-ST-U-90 is 6.98 mm, 10.92 mm, and 8.04 mm corresponding to the failure load of 116 kN, 146 kN, and 124 kN respectively. Whereas in control specimen S0-0L, the maximum deflection is 6.44 mm corresponding to 100 kN failure load. It is also observed that the midspan deflection of beams, strengthened with GFRP strips is less in comparison to the control specimen for the same load. In S300 series, the maximum deflection of strengthened beams S300-1L-ST-S-90, S300-1L-ST-S-45, and S300-1L-ST-U-90 is 10.75 mm, 11.94 mm, and 11.28 mm corresponding to the failure load of 154 kN, 166 kN, and 164 kN respectively, whereas in control beam specimen the value is 9.71 mm corresponding to the failure load of 140 kN. In series S0 and S300, the beam strengthened with GFRP strips on side of the web of the T-beams, with orientation of the strip at 45˚ to the longitudinal axis of the beam, carry more loads and also demonstrate more ductility than the others. In S200 series, the maximum deflection of beam strengthened with GFRP strips for S200-1L-ST-S-90, S200-1L-ST-S-45, and S200-1L-ST-U-90 is 12.75 mm, 14.51 mm, and 14.34 mm corresponding to the failure load of 172 kN, 182 kN, and 186 kN respectively, whereas in control beam specimen (S200-0L) the value is 9.98 mm corresponding to the failure load of 150 kN. As expected the beam strengthened with GFRP strips on side of the web of the T-beams at 45° orientation to the longitudinal axis of the beam show slightly more deflection than the other two. It is also observed that as transverse steel reinforcement increases, the deflection of the strengthened beam increases from S0 series to S200 series.

4.3 Cracking pattern and modes of failure

The cracking pattern and modes of failure of strengthened RC T-beams of S0, S300, and S200 series is shown in Fig. 8. In specimens S0-1L-ST-S-90, S0-1L-ST-S-45, and S0-1L-ST-U-90 of series S0, the diagonal shear crack initiated between a loads of 70 to 80 kN. As load increases, the crack propagated in a similar manner of specimen S0-0L. The failure is caused due to debonding of GFRP strips in specimen S0-1L-ST-S-90 over the main diagonal shear crack at an ultimate load of 116 kN, whereas in S0-1L-ST-S-45 and S0-1L-ST-U-90 specimens the failure is caused due to rupture and debonding of the GFRP strip from the concrete surface at an ultimate load of 146 kN and 124 kN respectively. In series S300, the diagonal shear crack initiated at a load of 90 kN in the specimens S300-1L-ST-S-90, S300-1L-ST-S-45, and S300-1L-ST-U-90. Thereafter, as load
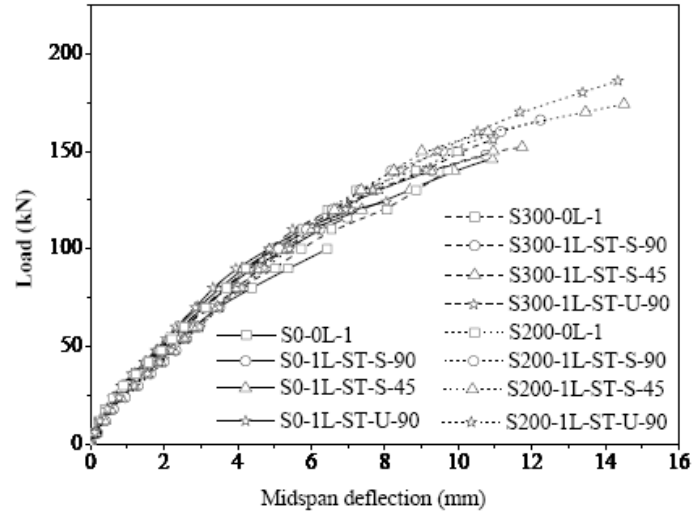
Fig. 7 Load versus midspan deflection for S0, S300 and S200 series

increases, the width of the crack is also increases. At the same time the GFRP strip, which crosses the shear crack, is also increases. In S300-1L-ST-S-90 specimen, the ultimate failure of the beam is caused due to debonding of the GFRP strips at a load of 154 kN. In S300-1L-ST-S-45 and S300-1L-ST-U-90 specimens, the ultimate failure of the beam is attained at a load of 166 kN and 164 kN respectively. The failure is caused due to rupture and debonding of the GFRP strips. Similarly in S200 series, the diagonal shear crack initiated at a load of 110 kN in the specimens S200-1L-ST-S-90, S200-1L-ST-S-45, and S200-1L-ST-U-90 respectively. As load increased, the width of the crack is also increased. The failure of the GFRP strips is caused mainly due to debonding of the GFRP strips from the concrete surface in specimens S200-1L-ST-S-90 at a load of 172 kN. Whereas in S200-1L-ST-S-45 and S200-1L-ST-U-90 specimens, the failure of the beam is caused due to debonding and rupture of the GFRP strips at a load of 182 kN and 186 kN respectively.

4.4 Strain in GFRP strips

The developed vertical strains in GFRP strip due to shear force for different configuration and orientation of GFRP strips in S0, S300, and S200 series are shown in Figs. 9-11. The strain in the GFRP strips in all the strain gauges did not contribute to the shear carrying capacity at the initial stages of loading. In series S0, specimen S0-1L-ST-S-90, the strain in the GFRP strip in most of the strain gauges started increasing between 40 kN to 45 kN shear force approximately. Thereafter, as shear force increases, the strain suddenly increases and attained the maximum value of 8884 μstrains at 58 kN shear force. Whereas in specimen S0-1L-ST-S-45 the strain in the GFRP strip started increasing in all the strain gauges between 40 kN to 50 kN shear force. The maximum strain observed 9932 μstrains at 70 kN shear force. In S0-1L-ST-U-90 specimen, the strain in the GFRP strip started increasing after 35 kN shear force, and attained the maximum value of 9076 μstrains at 62 kN shear force. In series S0, the strain is higher in the specimens strengthened the GFRP strip on side of the web of the T-beams at 45° orientation to the longitudinal axis of the beam, whereas in 90° orientation the strain is less.

K.C. Panda, S.K. Bhattacharyya and S.V. Barai

(a) Failure Modes of Tested Beams - Series-S0 (Strips)

(b) Failure Modes of Tested Beams - Series-S300 (Strips)

(c) Failure Modes of Tested Beams - Series-S200 (Strips)

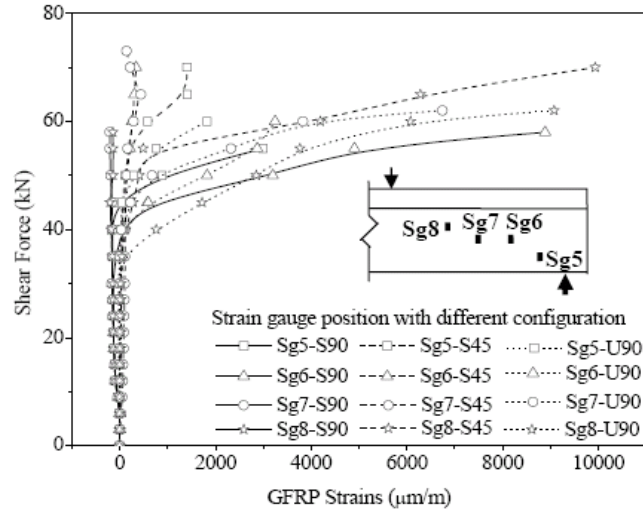Fig. 8 Modes of failure of tested beams

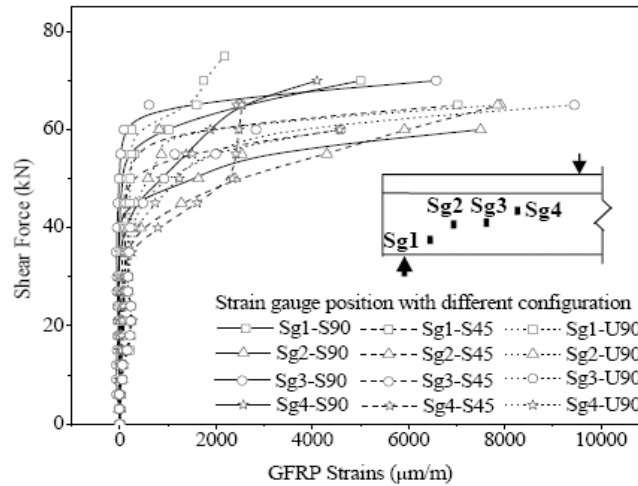Fig. 9 Shear force versus strain in GFRP strips of series S0

Fig. 10 Shear force versus strain in GFRP strips of series S300

The same trend is also observed in series S300 and S200. In series S300 and S200, the strain in the GFRP strip in all the strain gauges did not contribute to the shear carrying capacity approximately between 35 kN to 40 kN shear force and 40 kN to 50 kN shear force respectively. As shear force increases, the strain increases suddenly in S300-1L-ST-S-90, and S300-1L-ST-S-45 specimens and attained the maximum value 7497 μstrains at 60 kN shear force and 7917 μstrains at 65 kN shear force respectively. Whereas in S300-1L-ST-U-90 specimen the strain increases slowly up to 50 kN shear force, thereafter the shear force increases suddenly and attained the maximum value of 9450 μstrains at 65 kN shear force. In series S300, the maximum strain is observed in RC T-beams strengthened with GFRP strips in U-shape, whereas in side bonded, the strain is higher in the specimen strengthened the GFRP strips on side of the web of the T-beams at 45° to the longitudinal axis of the beam.
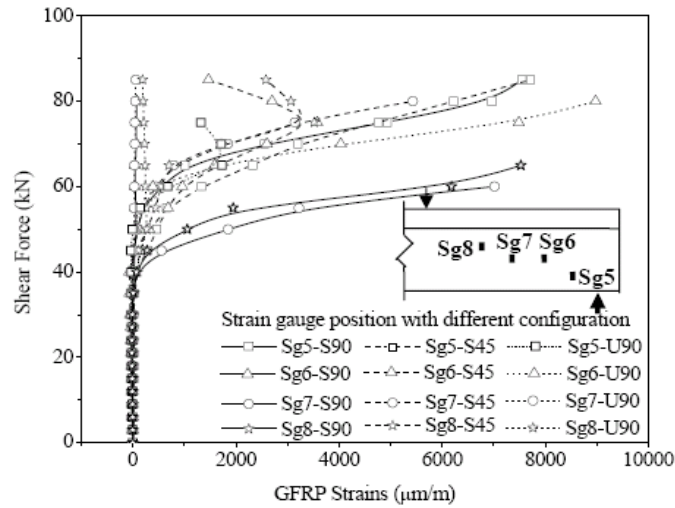
Fig. 11 Shear force versus strain in GFRP strips of series S200

In series S200, the maximum strain in S200-1L-ST-S-90 specimen is measured 7548 μstrains at 85 kN shear force in Sg5 strain gauge. Whereas in S200-1L-ST-S-45 and S200-1L-ST-U-90 specimens the value is 7716 μstrains at 85 kN shear force, and 8978 μstrains at 80 kN shear force respectively. In series S200, the maximum strain is observed in U-shape strengthened beam. Whereas in side bonded strengthened beams, the maximum strain is observed in 45°orientations of GFRP strips.

It may be concluded that, without shear reinforcement (S0 series) the strain is higher in the beam strengthened with inclined GFRP strips at 45°orientation to the longitudinal axis of the beam, whereas with shear reinforcement (for S300 and S200 series), the strain is higher in the beam strengthened with U-bonded GFRP strips. It indicates that the combination of shear reinforcement and anchorage of GFRP strips gives higher strain.

4.5 Strain in transverse steel

The curves representing the shear force versus the strains in the transverse steel reinforcement of series S200 and S300 for strain gauge ISg3 and ISg2 is shown in Figs. 12-13. It is observed that, the transverse steel reinforcement did not contribute to the shear carrying capacity at the initial stage of loading. This contribution is more effective after the diagonal cracking. In the control specimen S200-0L, and strengthened specimens S200-1L-ST-S-90, and S200-1L-ST-U-90, it occurred between 35 to 40 kN shear force. Whereas in specimen S200-1L-ST-S-45 the contribution is effective from the beginning and shows lesser value up to 40 kN shear force. Thereafter, the strain in the transverse steel in the entire strengthened beam gets increased with the increase in shear forces. The maximum strain observed in control specimen is 1983 μstrains at 60 kN shear force, whereas the strain in strengthened beams corresponding to this shear force is 1905 μstrains, 1152 μstrains, 624 μstrains in S200-1L-ST-S-90, S200-1L-ST-S-45, and S200-1L-ST-U-90 respectively. The maximum strain is also observed in S200-1L-ST-S-90, S200-1L-ST-S-45, and S200-1L-ST-U-90 specimens are 2606 μstrains at 65 kN shear force and 1864 μstrains, and 1422 μstrains at 75 kN shear force respectively.
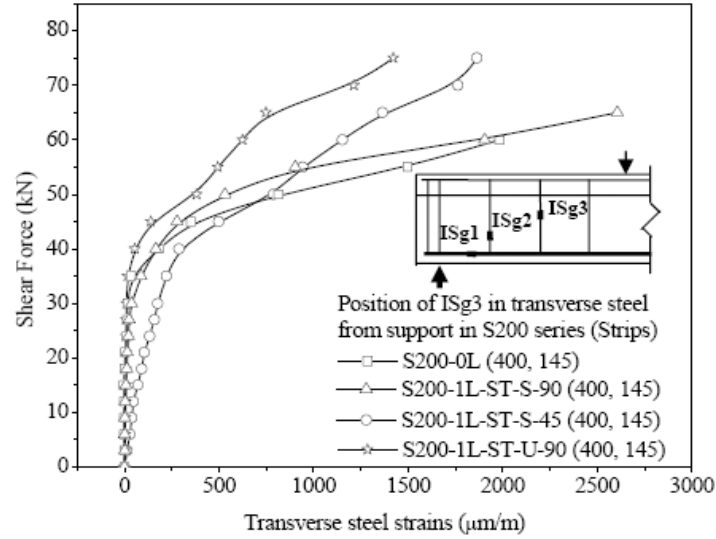
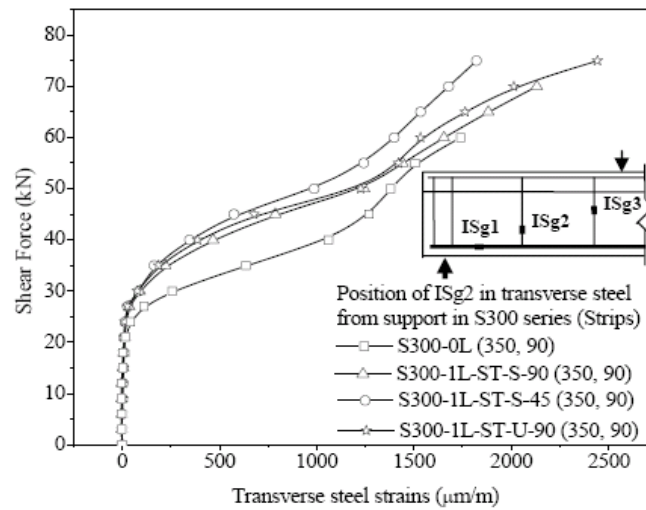Fig. 12 Shear force versus strain in the transverse steel of series S200

Fig. 13 Shear force versus strain in the transverse steel of series S300

In series S300, in the control specimen S300-0L, the contribution of transverse steel to the shear carrying capacity is occurred approximately after 25 kN shear force, whereas for the strengthened specimens S300-1L-ST-S-90, S300-1L-ST-S-45, and S300-1L-ST-U-90 it occurred between the shear force of 25 to 30 kN. Thereafter, as shear force increases, the strain in the transverse steel increases. In control specimen the maximum strain is observed 1740 μstrains at 60 kN shear force, whereas the strain in strengthened beams corresponding to this shear force is 1654 μstrains, 1534 μstrains, 1398 μstrains in S300-1L-ST-S-90, S300-1L-ST-U-90, and S300-1L-ST-S-45 respectively. The maximum strain is also observed in strengthened beams 2132 μstrains at 70 kN shear force, and 1822 μstrains, and 2443 μstrains at 75 kN shear force respectively.
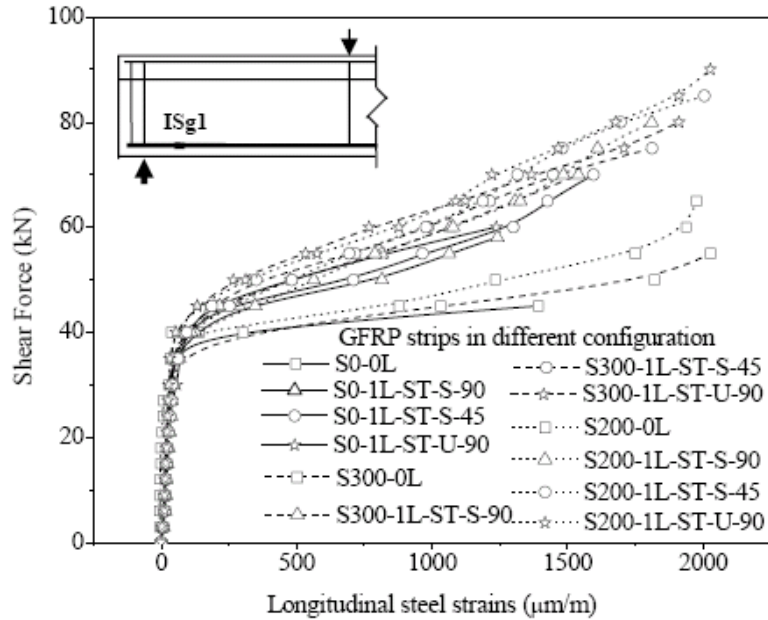
Fig. 14 Shear force versus strain in the longitudinal steel of all series

It is observed that, the strain in the transverse steel is less in strengthened beams as compared to the control beam for the same amount of shear force. So far as the configuration is concerned, the strain in the transverse steel with U-shape GFRP strips is less as compared to the side bonded GFRP strips for S200 series, whereas in S300 series it is more as compared with the diagonal side strips.

4.6 Strain in longitudinal steel

The curves representing the shear force versus the strains in the longitudinal steel reinforcement for different configuration of GFRP strips of series S0, S200 and S300 is shown in Fig. 14. The strain in the longitudinal steel near the support point is very small at the initial stages of loading. As shear force increases, the strain increases linearly up to about 35 kN shear force as the diagonal shear cracks appear in the concrete. After the appearance of diagonal shear cracks in the concrete, the longitudinal steel reinforcement resists the further increments of shear force. In series S0, in control specimen S0-0L, the strain suddenly increases after 35 kN shear force, and attained the maximum value of 1392 μstrains at 45 kN shear force. Whereas in strengthened beams S0-1L-ST-S-90, S0-1L-ST-S-45, and S0-1L-ST-U-90, the strain corresponding to this shear force are 288 μstrains, 215 μstrains, and 176 μstrains respectively. Thereafter, as shear force increases, the strain increases suddenly in strengthened beams and attained the maximum value of 1242 μstrains at 58 kN shear force, 1596 μstrains at 70 kN shear force, and 1238 μstrains at 60 kN shear force in S0-1L-ST-S-90, S0-1L-ST-S-45, and S0-1L-ST-U-90 respectively. In series S300, in control specimen S300-0L, the strain suddenly increases after 35 kN shear force, and attained the maximum value of 2028 μstrains at 55 kN shear force. Whereas in strengthened beam S300-1L-ST-S-90, S300-1L-ST-S-45, and S300-1L-ST-U-90, the strain corresponding to this shear force

are 815 μstrains, 717 μstrains, and 534 μstrains respectively. Thereafter, as load increases, the strain increases gradually in strengthened beams and attained the maximum value of 1541 μstrains at 70 kN shear force, 1813 μstrains at 75 kN shear force, and 1912 μstrains at 80 kN shear force in S300-1L-ST-S-90, S300-1L-ST-S-45, and S300-1L-ST-U-90 respectively. In series S200, in control specimen S200-0L, the strain suddenly increases after 35 kN shear force, and attained the maximum value of 1976 μstrains at 65 kN shear force. Whereas in strengthened beams S200-1L-ST-S-90, S200-1L-ST-S-45, and S200-1L-ST-U-90, the strain corresponding to this shear force are 1327 μstrains, 1188 μstrains, 1088 μstrains respectively. Thereafter, as load increases, the strain increases gradually in strengthened beams and attained the maximum value of 1812 μstrains at 80 kN shear force, 2006 μstrains at 85 kN shear force, and 2028 μstrains at 90 kN shear force in S200-1L-ST-S-90, S200-1L-ST-S-45, and S200-1L-ST-U-90 respectively.

It is observed that, the strain in the longitudinal steel, in beams strengthened with GFRP strips is less as compared with the control beam specimen for the same amount of shear force in all the series. As configuration of GFRP strips is concerned, the strain in the longitudinal steel in beam strengthened with U-shape GFRP strips is less as compared to the side bonded GFRP strips for the same amount of shear force. It is also expected that, as transverse steel reinforcement increases, the longitudinal steel is less strained for the same amount of shear force.

5. Comparison of test results with ACI predictions

Table 6 shows a comparison between the experimental results of GFRP strengthened RC T-beams and shear resistance results calculated based on ACI code (ACI 440.2R-02). The column $(V_{f,test} / V_{n,test,ref}) \times 100\%$ indicates the percentage of increase in strength of the GFRP strip of the strengthened beam specimen with respect to the corresponding control specimen of three series S0-0L, S300-0L, and S200-0L. Let's take, $V_{f,test}$ of S0-1L-ST-S-90 specimen is 8 kN, $V_{n,test,ref}$ of S0-0L specimen is 50 kN. The contribution of GFRP strip to the shear carrying capacity is 16%. Theoretically, the shear strength contribution of concrete, transverse steel reinforcement and GFRP strip is calculated by using the ACI guidelines. The values are presented in Table 6.

Table 6 Comparison of experimental and ACI predicted shear resistance results

Specimen Designation	Experimental results						Theoretical results predicted by ACI 440.2R-02 Design approach				
	Load at failure (kN)	$V_{n,test}$ (kN)	$V_{c,test}$ (kN)	$V_{s,test}$ (kN)	$V_{f,test}$ (kN)	$\dfrac{V_{f,test}}{V_{n,test,rif}} \times$ 100 (%)	$V_{f,theor}$ (kN)	$V_{c,theor}$ (kN)	$V_{s,theor}$ (kN)	$\phi V_{n,theor}$ (kN)	$\dfrac{V_{f,test}}{V_{f,theor}}$
S0-0L	100	50	50	0	0	0	0	26.68	0	22.68	-
S300-0L	141	70.5	50	20.5	0	0	0	25.95	10.60	31.07	-
S200-0L	160	80	50	30	0	0	0	26.82	15.90	36.31	-
S0-1L-ST-S-90	116	58	50	0	08	16	3.13	26.09	0	24.44	2.56
S0-1L-ST-S-45	146	73	50	0	23	46	5.20	26.09	0	25.93	4.42
S0-1L-ST-U-90	124	62	50	0	12	24	3.13	26.09	0	24.44	3.83

Table 6 Continued

S300-1L-ST-S-90	154	77	50	20.5	6.5	9.22	3.13	25.59	10.60	33.02	2.08
S300-1L-ST-S-45	166	83	50	20.5	12.5	17.73	5.20	25.59	10.60	34.52	2.40
S300-1L-ST-U-90	164	82	50	20.5	11.5	16.31	3.13	25.59	10.60	33.02	3.67
S200-1L-ST-S-90	172	86	50	30	06	7.5	3.13	25.45	15.90	37.41	1.91
S200-1L-ST-S-45	182	91	50	30	11	13.75	5.20	25.45	15.90	38.90	2.11
S200-1L-ST-U-90	186	93	50	30	13	16.25	3.13	25.45	15.90	37.41	4.15

It may be observed the shear strength contribution of GFRP strips from the experimental investigation result ($V_{f,test}$) gives higher value as compared with the theoretical value ($V_{f,theor}$) calculated as per ACI guidelines (ACI 440.2R-02). The ratio, ($V_{f,test}/V_{f,theor}$) value for S0-1L-ST-S-45, S300-1L-ST-S-45, and S200-1L-ST-S-45 is 4.42, 2.40 and 2.11 respectively. It indicates as transverse steel reinforcement increases the ratio ($V_{f,test}/V_{f,theor}$) value decreases. Similar trend is also observed in strengthened beam with side shape GFRP strips and orientation of the strip at 90° to the longitudinal axis of the beam. Whereas in U-bonded GFRP strips the value for S0-1L-ST-U-90, S300-1L-ST-U-90, and S200-1L-ST-U-90 is 3.83, 3.67 and 4.15 respectively. It is observed that all experimental results are overestimating the ACI guidelines. It is observed that the shear strength contribution of GFRP strips from the experimental investigation is significantly decreases as transverse steel reinforcement increases, whereas in ACI design approach, the value is remains same for all variation of transverse steel reinforcements. However, the influence of the transverse steel on the contribution of GFRP strips to the shear resistance, although clearly demonstrated by tests, is not reflected in the guidelines since the shear resistance due to GFRP is the same, regardless of the presence of transverse steel.

6. Conclusions

This paper presents the results of an experimental investigation carried out on eighteen full scale simply supported RC T-beams strengthened in shear with externally bonded GFRP strips, in three series, with and without the transverse steel reinforcement. The test results clearly indicate that for strengthened RC T-beams in shear with side bonded and U-shaped GFRP strips increase the effectiveness by 7.5% to 46%.

1. The gain in shear capacity is significant in all the RC T-beams strengthened in shear with GFRP strips. As configuration and orientation is concerned, U-shape and side bonded with orientation of the strip at 45° to the longitudinal axis of the beam is more effective than side bonded with orientation of the GFRP strip at 90°.

2. The modes of failure of strengthened RC T-beams in shear with side bonded GFRP strips clearly indicate that, the strip at 90° to the longitudinal axis of the beam fails due to GFRP debonding, whereas for 45° orientations and U-shaped GFRP strip the fails is due to both GFRP

rupture and debonding.

3. The load-strain curves clearly indicates that, for S200 and S300 series, the combination of transverse steel and configurations and orientations resulted in the more utilization of GFRP strain, and attained the maximum strain in strengthened RC T-beams.

4. The addition of internal transverse steel resulted in a significant decrease in shear capacity of the GFRP strips oriented in 45° direction as compared with no transverse steel reinforcements. Whereas in U-shape and side shape with orientation of the GFRP strip at 90°, the decrease in shear capacity is less as compared with no transverse steel reinforcement.

5. The load-deflection graph clearly indicates that the RC T-beams strengthened in shear with GFRP strips have a significant effect on beams ductility. The RC T-beams, becomes more flexible and more deformable, after strengthened by GFRP strips.

6. The transverse steel is more strained in control specimens, as compared with strengthened specimens. This indicates that the addition of GFRP strips reduces the strain in transverse steel. As far as configuration of GFRP strips is concerned, the U-shape of GFRP strip resulted in an additional decrease of strains in the transverse steel reinforcement as compared with side bonded GFRP strip. As far as side bonded orientation is concerned, the strain in the transverse steel at 45° orientation of GFRP strip with the longitudinal axis of the beam is less as compared with 90° orientation of GFRP strip.

7. The longitudinal steel is more strained in control specimens, as compared with strengthened specimens. As far as configuration of GFRP strips is concerned, U-shape GFRP strips resulted in a decrease of strains in the longitudinal steel reinforcement as compared with side bonded GFRP strips. Also as far as orientation is concerned, the strain in the longitudinal steel at 45° orientation of GFRP strip is less as compared with 90°orientation of GFRP strip.

Acknowledgments

References

American Concrete Institute (ACI) (2002), "Building code requirements for reinforced concrete (ACI 318-02) and commentary", *318RM-02*, Detroit.

ACI 440.2R-02 (2002), "Guide for the design and construction of externally bonded FRP systems for strengthening concrete structures", *ACI Committee 440*, Farmington Hills, Michigan.

Al-Sulaimani, G.J., Sharif, A., Basunbul, I.A., Baluch, M.H. and Ghaleb, B.N. (1994), "Shear repair for reinforced concrete by fibreglass plate bonding", *ACI Struct. J.*, **91**(3), 458-464.

Adhikary, B.B., Mutsuyoshi, H. and Ashrof, M. (2004), "Shear strengthening of reinforced concrete beams using fibre reinforced polymer sheets with bonded anchorage", *ACI Struct. J.*, **101**(5), 660-668.

Belarbi, A., Bae, S. and Brancaccio, A. (2012), "Behavior of full-scale RC T-beams strengthened in shear with externally bonded FRP sheets", *Construction and Building Materials*, **32**, 27-40.

Berset, J.D. (1992), "Strengthening of reinforced concrete beams for shear using FRP composites", MS Thesis, Dept. of Civil and Environmental Engineering, MIT.

Bousselham, A. and Chaallal, O. (2004), "Shear strengthening reinforced concrete beams with fibre-reinforced polymer: assessment of influencing parameters and required research", *ACI Struct. J.*, **101**(2), 219-227.

Bousselham, A. and Chaallal, O. (2006), "Effect of transverse steel and shear span of the performance of RC beams strengthened in shear with CFRP", *Composites: Part B*, **37**, 37-46.

Bousselham, A. and Chaallal, O. (2006), "Behavior of reinforced concrete T-beams strengthened in shear with carbon fibre reinforced polymer - An experimental study", *ACI Struct. J.*, **103**(3), 339-347.

Bousselham, A. and Chaallal, O. (2008), "Mechanisms of shear resistance of concrete beams strengthened in shear with externally bonded FRP", *J. Compos. Constr.*, **12**(5), 499-512.

Cao, S.Y., Chen, J.F., Teng, J.G., Hao, Z. and Chen, J. (2005), "Debonding in RC beams shear strengthened with complete FRP wraps", *J. Compos. Constr.*, **9**(5), 417-428.

Chaallal, O., Nollet, M.J. and Perraton, D. (1998), "Shear strengthening of RC beams by externally bonded side CFRP strips", *J. Compos. Constr.*, **2**(2), 111-113.

Chaallal, O., Shahawy, M. and Hassan, M. (2002), "Performance of reinforced concrete T-Girders strengthened in shear with carbon fibre-reinforced polymer fabric", *ACI Struct. J.*, **99**(3), 335-343.

Chajes, M.J., Januszka, T.F., Mertz, D.R., Thomson, T.A., Jr. and Finch, W.W., Jr. (1995), "Shear strengthening of reinforced concrete beams using externally applied composite fabrics", *ACI Struct. J.,* **92**(3), 295-303.

Chen, J.F. and Teng, J.G. (2003a), "Shear capacity of FRP-strengthened RC beams: FRP debonding", *Constr. Build. Mater.*, **17**(1), 27-41.

Chen, J.F. and Teng, J.G. (2003b), "Shear capacity of fibre-reinforced polymer strengthened RC beams: Fibre reinforced polymer rupture", *J. Struct. Eng.*, **129**(5), 615-625.

Chen, G.M., Teng, J.G. and Chen, J.F. (2010a), "RC beams shear strengthened with FRP: shear resistance contributed by FRP", *Mag. Concrete. Research*, **62**, 301-311.

Chen, G.M., Teng, J.G., Chen, J.F. and Rosenboon, O.A. (2010b), "Interaction between steel stirrups and shear strengthening FRP strips in RC beams", *J. Compos. Constr.*, **14**, 498-509.

Chen, G.M., Teng, J.G. and Chen, J.F. (2012), "process of debonding in RC beams shear-strengthened with FRP U-strips or side strips", *International Journal of Solids and Structures*, **49**, 1266-1282.

Deniaud, C. and Cheng, J.J.R. (2001), "Shear behavior of reinforced concrete T-beams with externally bonded fibre-reinforced polymer sheets", *ACI Struct. J.*, **98**(3), 386-394.

Deniaud, C. and Cheng, J.J.R. (2003), "Reinforced concrete T-beams strengthened in shear with fibre reinforced polymer sheets", *J. Compos. Constr.*, **7**(4), 302-310.

Egilmez. O. O. and Yormaz. D. (2011), "Cyclic testing of steel I-beams reinforced with GFRP", *Steel and Compos. Struct.*, **11**(2), 93-114.

EI-Ghandour, A.A. (2011), "Experimental and analytical investigation of CFRP flexure and shear strengthening efficiencies of RC beams", *Construction and Building Materials*, **25**, 1419-1429.

Indian Standard (IS) (2000), "Plain and reinforce concrete code of practice IS 456:2000", India.

Hag-Elsafi, O., Alampalli, S. and Kunin J. (2001), "Application of FRP laminates for strengthening of a reinforced-concrete T-beam bridge structure", *Composite Structures*, **52**(3-4), 453-466.

Khalifa, A., Gold, W.J., Nanni, A. and Aziz, A. (1998), "Contribution of externally bonded FRP to shear capacity of RC flexural members", *J. Compos. Constr.*, **2**(4), 195-201.

Khalifa, A. and Nanni, A. (2000), "Improving shear capacity of existing RC T-section beams using CFRP composites", *Cement and Concrete Composites*, **22**, 165-174.

Khalifa, A.and Nanni, A. (2002), "Rehabilitation of rectangular simply supported RC beams with shear deficiencies using CFRP composites", *Construction and Building Materials*, **16**, 135-146.

Kim, G., Sim, J. and Oh, h. (2008), "Shear strength of strengthened RC beams with FRPs in shear", *Construction and Building Materials*, **22**, 1261-1270.

Lee, T.K. and Al-Mahaidi, R. (2008), "An experimental investigation on shear behaviour of RC T-beams strengthened with CFRP using photogrammetry", *Composite Structures*, **82**(2), 185-193.

Lee, H.K., Cheong, S.H., Ha, S.K. and Lee, C.G. (2011), "Behavior and performance of RC T-section deep beams externally strengthened in shear with CFRP sheets", *Composite Structures*, **93**(2), 911-922.

Leung, C.K.Y., Chen, Z., Lee, S., Ng, M., Xu, M. and Tang, J. (2007), "Effect of size on the failure of geometrically similar concrete beams strengthened in shear with FRP strips", *J. Compos. Constr.*, **11**(5), 487-496.

Li, A., Assih, J., and Delmas, Y. (2001), "Shear strengthening of RC beams with externally bonded CFRP sheets", *J. Struct. Eng.*, **127**(4), 374-380.

Li, A., Diagana, C. and Delmas, Y. (2002), "Shear strengthening effect by bonded composite fabrics on RC beams", *Composites: Part B*, **33**, 225-239.

Maaddawy, T.E. and Sherif, S. (2009), "FRP composites for shear strengthening of reinforced concrete deep beams with openings", *Composite Structures*, **89**, 60-69.

Maeda, T., Asano, Y., Sato, Y., Ueda, T., and Kakuta, Y. (1997), "A study on bond mechanism of carbon Fibre sheet", *Non-Metallic (FRP) Reinforcement for Concrete Structures: Proceedings of the Third International Symposium on Non-Metallic (FRP) Reinforcement for Concrete Structures*, **1**, Japan Concrete Institute, Tokyo, Japan.

Malek, A.M. and Saadatmanesh, H. (1998), "Ultimate shear capacity of reinforced concrete beams strengthened with web-bonded fiver-reinforced plastic plates", *ACI Struct. J.*, **95**(4), 391-399.

Micelli, F., Anniah, R.H. and Nanni, A. (2002), "Strengthening of short shear span reinforced concrete T joists with fibre reinforced plastic composites", *J. Compos. Constr.*, **6**(4), 264-271.

Monti, G. and Liotta, M.A. (2007), "Tests and design equations for FRP-strengthening in shear", *Construction and Building Materials*, **21**, 799-809.

Mosallam, A.S. and Banerjee, S. (2007), "Shear enhancement of reinforced concrete beams strengthened with FRP composite laminates", *Composites: Part B*, **38**, 781-793.

Noris, T., Saadatmanesh, H. and Ehsani, M.R. (1997), "Shear and flexural strengthening of RC beams with carbon fibre sheets**",** *J. Struct. Eng.***,** **123**(7), 903-911.

Panda, K.C., Bhattacharyya, S.K. and Barai, S.V. (2010), "Shear behaviour of reinforced concrete T-beams with U-bonded glass fibre reinforced plastic sheet", *The Indian Concrete Journal*, **84**(10), 61-71.

Panda, K.C., Bhattacharyya, S.K. and Barai, S.V. (2011), "Shear strengthening of RC T-beams with externally side bonded GFRP sheet", *J. Reinforced Plastic and Composites*, **30**(13), 1139-1154.

Panda, K.C., Bhattacharyya, S.K., and Barai, S.V. (2012), "Shear behaviour of RC T-beams strengthened with U-wrapped GFRP sheet", *Steel and Composite Structures*, **12**(2), 149-166.

Panda, K.C., Bhattacharyya, S.K., and Barai, S.V. (2013), "Effect of transverse steel on the performance of RC T-beams strengthened in shear zone with GFRP sheet", *Construct. Build. Mater.*, **41**, 79-90.

Pellegrino, C. and Modena, C. (2002), "Fibre reinforced polymer shear strengthening of reinforced concrete beams with transverse steel reinforcement", *J. Compos. Constr.*, **6**(2), 104-111.

Sundarraja, M.C. and Rajamohan, S. (2009), "Strengthening of RC beams in shear using GFRP inclined strips - An experimental study", *Construction and Building Materials*, **23**, 856-864.

Taljsten, B. and Elfgren, L. (2000), "Strengthening concrete beams for shear using CFRP-materials: evaluation of different application methods", *Composites Part B: Engineering*, **31**, 87-96.

Taljsten, B. (2003), "Strengthening concrete beams for shear with CFRP sheets", *Constr. Build. Mater.,* **17**(1), 15-26.

Triantafillou, T.C. (1998), "Shear strengthening of reinforced concrete beams using epoxy bonded FRP composites", *ACI Struct. J.*, **95**(2), 107-115.

Triantafillou, T.C. and Antonopolous, C.P. (2000), "Design of concrete flexural members strengthened in shear with FRP", *J. Compos. Constr.*, **4**(4), 198-205.

Zhang, Z. and Hsu, C.T.T. (2005), "Shear strengthening of reinforced concrete beams using carbon-fibre-reinforced polymer laminates", *J. Compos. Constr.*, **9**(2), 158-169.

Notations

The following symbols are used in this paper:

a = shear span, mm

A_c = area of concrete cross section, mm^2

A_f = area of GFRP external shear reinforcement = $2t_f w_f$, mm^2

A_{sl} = total area of longitudinal steel reinforcement, mm^2

A_{sw} = total area of transverse steel reinforcement, mm^2

b_w = width of the beam cross-section, mm

d = depth from the top of the section to the centre of tension steel reinforcement, mm

d_f = effective depths of GFRP shear reinforcement, mm

E_f = elastic modulus of GFRP, GPa

E_s = elastic modulus of steel reinforcement, GPa

s_f = spacing of GFRP strips, mm

t_f = thickness of GFRP sheet on one side of the beam, mm

$V_{c,test}$ = nominal shear strength provided by concrete (experimental value)

$V_{c,theor}$ = nominal shear strength provided by concrete (theoretical value)

$V_{f,test}$ = nominal shear strength provided by GFRP shear reinforcement (experimental value)

$V_{f,theor}$ = nominal shear strength provided by GFRP shear reinforcement (theoretical value)

$V_{n,test}$ = nominal shear strength (experimental value)

$V_{n,theor}$ = nominal shear strength (theoretical value)

$V_{s,test}$ = nominal shear strength provided by steel shear reinforcement (experimental value)

$V_{s,theor}$ = nominal shear strength provided by steel shear reinforcement (theoretical value)

w_f = width of GFRP strips, mm

ε_{fe} = effective strain in GFRP sheet

ε_{fu} = ultimate tensile strain of fibre material in the GFRP composite

ϕ = strength reduction factor

ρ_f = GFRP shear reinforcement ratio = $(2t_f / b_w)(w_f / s_f)$

ρ_s = transverse steel reinforcement ratio = $A_{sw} /(sb_w)$

ρ_w = Longitudinal steel reinforcement ratio = $A_{sl} /(b_w d)$